A dielectrophoresis-based microchannel system

X. X. Zhao,[a] Y. Gao, and J. P. Huang[b]
Surface Physics Laboratory (National Key Laboratory) and Department of Physics, Fudan University, Shanghai 200433, People's Republic of China

(Received 1 October 2008; accepted 5 February 2009; published online 23 March 2009)

In this paper, we will propose a dielectrophoresis-based microchannel system. Based on numerical calculations and theoretical analysis, we investigate the dynamic behaviors of a microparticle in this system, in the presence of nonuniform electric fields generated by point microelectrodes. Good agreement is shown between them. It is found that the microelectrodes enable the system equilibrium to shift between monostable and bistable states. Further, we reveal that the microparticle can oscillate along the microchannel with a fixed period for the ideal case without a drag force, and that it can be located in either monostable or bistable states for the cases with drag forces. In view of these findings, we carefully address the possibility to design several microfluidic devices, namely, a microparticulate clock for timing, a binary random number generator for conducting stochastic calculations, and a flip-flop device for system memory. © *2009 American Institute of Physics*. [DOI: 10.1063/1.3093919]

I. INTRODUCTION

Lab-on-a-chip (LOC) is a term for devices that integrate multiple laboratory functions on a single chip of only millimeters to a few square centimeters in size and that are capable of handling extremely small fluid volumes down to less than picoliters.[1–3] For LOC systems, device designs are always a hot topic, which require a high degree of integration, a small scale of dimension, and a fast analysis speed. Thorsen *et al.*[4] designed a microfluidic memory storage device with 1000 independent compartments and 3574 microvalves, organized as an addressable 25×40 chamber microarray. Ramsey *et al.*[5] achieved 80 nm for microchannel depth, which reduces the volume of samples to even picoliter. Until now, function units for LOC systems include various aspects, such as micropumps, microreactors, microseparators, microanalytical devices, and microcontrol units (e.g., logic gates[6,7] and microtimers[7]). However, existing reports on multifunctional devices remain limited. On the other hand, dielectrophoresis is gaining increasing attention for its capability of manipulating uncharged particles, and its noninvasive and nondestructive property makes it useful method in LOC systems.[8–22] In this work, we propose a dielectrophoresis-based microchannel system, and investigate intriguing dielectrophoresis-based behaviors of a microparticle in it. The nonuniform electric field for manipulating the microparticle is achieved by three triangularly situated microelectrodes. Our analysis demonstrates that it is possible to design several microfluidic devices based on this system, which potentializes it as a multifunctional unit for LOC systems. The limitations arising from our designs will also be carefully addressed.

[a]Electronic mail: zhaoxiaoxue.zxx@gmail.com.
[b]Author to whom correspondence should be addressed. Electronic mail: jphuang@fudan.edu.cn.

II. DIELECTROPHORESIS THEORY

Dielectrophoresis (DEP) describes the movement of particles under the influence of a nonuniform electric field.[8,23] For presenting the DEP theory used in this work, let us start by considering a lossless dielectric particle suspended in a lossless dielectric liquid in the presence of a nonuniform electric field. In such case, polarization charges accumulate on the interface between the particle and the liquid, due to the difference of their polarizations, which induce an electric moment in the particle. (In the sense of lossless particle and medium, conductivities for both are assumed to be pretty small and can be ignored, such that moment due to free charge accumulation can be ignored compared with polarization charge accumulation.) Then, the interaction between the moment and the external nonuniform electric field yields a net force acting on the particle. This force is just the DEP force. Throughout this work, only the dipolar moment will be taken into account. We will not consider any other higher-order moments (e.g., quadrupolar moments, octupolar moments, etc.). In fact, such higher-order moments can appear if the electric field nonuniformity is significant. In other words, we shall only consider the case in which the nonuniformity is so modest that the size of the particle could be much smaller than the characteristic dimension of the electric field nonuniformity. In this case, the dipolar interaction plays a dominant role, and the DEP force is denoted as $\mathbf{F}_{\mathrm{DEP}}=\mathbf{P}_{\mathrm{eff}}\cdot\nabla\mathbf{E}$,[23] where $\mathbf{P}_{\mathrm{eff}}$ is the effective dipole moment of the dielectric particle and $\nabla\mathbf{E}$ is the gradient of the external electric field vector $\mathbf{E}$. For a dielectric spherical particle with radius a, $\mathbf{P}_{\mathrm{eff}}$ is given by

$$\mathbf{P}_{\mathrm{eff}}=4\pi\varepsilon_1 a^3 K\mathbf{E}, \tag{1}$$

where $K\equiv(\varepsilon_2-\varepsilon_1)/(\varepsilon_2+2\varepsilon_1)$ is the Clausius–Mossotti factor, and ε_1 (or ε_2) is the permittivity of the liquid (or particle). Due to the lossless property for both particle and medium, their conductivities can be ignored, and real permit-

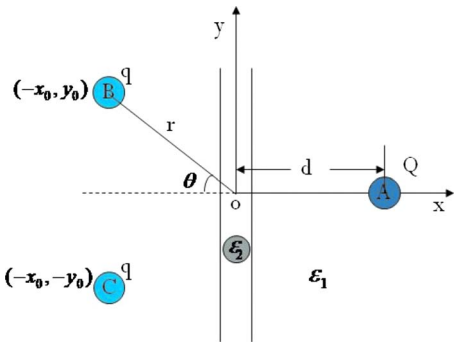

FIG. 1. (Color online) Schematic graph showing the microchannel system with three triangularly situated point microelectrodes A, B, and C. The center of the microchannel is denoted as O, which also serves as the origin of the Cartesian coordinates (x,y). Microelectrode A is situated on the x axis. Microelectrodes B and C are located at coordinates $(-x_0,y_0)$ and $(-x_0, -y_0)$, respectively. Microparticle P with permittivity ε_2 can only move along the y-directed microchannel. Q and q denote the charges applied on A and B (or C), respectively. d (or r) is the center-to-center distance between the microchannel and microelectrode A (or between the microchannel and microelectrode B or C). θ denotes the angle between the x axis and the line joining the centers of microelectrode B (or C) and the microchannel. ε_1 is used to denote the permittivity of both the medium inside or outside the microchannel and the material making the microchannel.

tivities prevail for both of them. Thus the DEP force acting upon the particle admits[8,23]

$$\mathbf{F}_{\mathrm{DEP}} = 2\pi\varepsilon_1 a^3 K \nabla E^2. \tag{2}$$

According to this equation, a suspended particle is either attracted to or repelled from a region with greater electric field intensity, determined by whether K is positive (namely, $\varepsilon_2 > \varepsilon_1$) or negative (i.e., $\varepsilon_2 < \varepsilon_1$). The former corresponds to "positive DEP" and the latter corresponds to "negative DEP."

III. THE MICROCHANNEL SYSTEM AND SOME PROPOSED APPLICATIONS

Let us consider a microchannel system with three triangularly situated point microelectrodes denoted by A, B, and C (see Fig. 1). B and C are located symmetrically about axis x on which A is positioned. Microparticle denoted by P is restricted along y-direction by the microchannel. For our work is only to establish a concept, we take ε_1 as the permittivity for both the medium inside or outside the microchannel and the material making the microchannel, so that the boundary effect can be ignored. In the mean time, the permittivity ε_2 of the microparticle is taken to be greater than ε_1, indicative of positive DEP (both the permittivities of the microparticle and the medium in the channel are real, for the lossless properties for both of them). The dimension of the microelectrodes is set to be much larger than the size of the microparticle, and thus the scale of the nonuniformity of the electric field is large compared to the dimension of the microparticle. In this regard, it is safe to apply Eq. (2) to calculate the DEP force acting on the microparticle. Different charge distributions on microelectrodes A, B, and C create different patterns of a nonuniform dc-electric field, based on which three applications are carefully addressed in Secs. III A–III C.

A. A microparticulate clock

Let us first consider the microchannel system with charge Q applied on A, and no charge applied on B or C. In this section, we shall only take into account the DEP force by neglecting all the other forces such as gravity, friction, and Brownian forces. Point microelectrode A with charge Q produces a Coulomb electric field, which further provides DEP force on the microparticle. The sum of force imposed on P is simply the y-direction component of the DEP force

$$\mathbf{F} = 2\pi\varepsilon_1 a^3 K \frac{\partial E^2}{\partial y}\hat{\mathbf{e}}_y = -\frac{a^3 Q^2 \varepsilon_1(\varepsilon_2-\varepsilon_1)y}{2\pi(d^2+y^2)^3\varepsilon_2^2(2\varepsilon_1+\varepsilon_2)}\hat{\mathbf{e}}_y. \tag{3}$$

For numerical calculations, we set $\varepsilon_1=\varepsilon_0$ (ε_0 is the permittivity of vacuum), and choose $\varepsilon_2=9\varepsilon_0$, $a=1$ μm, with mass density $\rho=3.75\times10^3$ kg/m^3. Such values can be realized by using an Al_2O_3 microparticle. Figure 2(a) displays the force F acting on microparticle P as a function of its displacement y, according to Eq. (2). The curve goes symmetrically about the origin through quadrants 2 and 4, demonstrating its restoring property. We can see that the system is a monostable system with the origin the equilibrium point.

To investigate the dynamic behavior of the microparticle in this system, we assume that the microparticle is initialized with a displacement from the origin. It is easy to understand that the microparticle will oscillate along the microchannel with a fixed period. For a small amplitude within the linear region, the oscillation of microparticle P is simply harmonic, for which we compare results by both theoretical and numerical calculations [Fig. 2(b)]. For the theoretical approach, we first perform the Taylor expansion to get the linear part k of the force F, and then obtain its oscillation trajectory by solving the equation

$$\frac{\mathrm{d}^2y}{\mathrm{d}t^2} + \omega^2 y = 0, \tag{4}$$

where $\omega=\sqrt{k/m}$ is the angular frequency of the oscillation. As for the numerical method, we let the initial displacement of the microparticle to be 5 μm, and solve numerically the equation

$$\frac{\mathrm{d}^2y}{\mathrm{d}t^2} = \frac{F}{m}, \tag{5}$$

in which F takes the form of Eq. (3). Figure 2(b) displays a good agreement between our theoretical and numerical methods. Then, in Fig. 2(c), we calculate the oscillation period T versus microelectrode parameters Q and d using both methods. Again it is clear that the theoretical and numerical results agree perfectly with each other. It is found that T is caused to monotonically decrease as the charge Q is increased or the distance d of microelectrode A is decreased. For larger displacements of microparticle P, the oscillation will not be simply harmonic, and the oscillation period T depends on the amplitude L [see Fig. 2(d)]. Figure 2(d) shows a monotonic increase in T when L increases, which is due to the important role of the nonlinear part of the force acting on microparticle P. The value for small amplitudes obtained theoretically is also marked for reference. It is clear

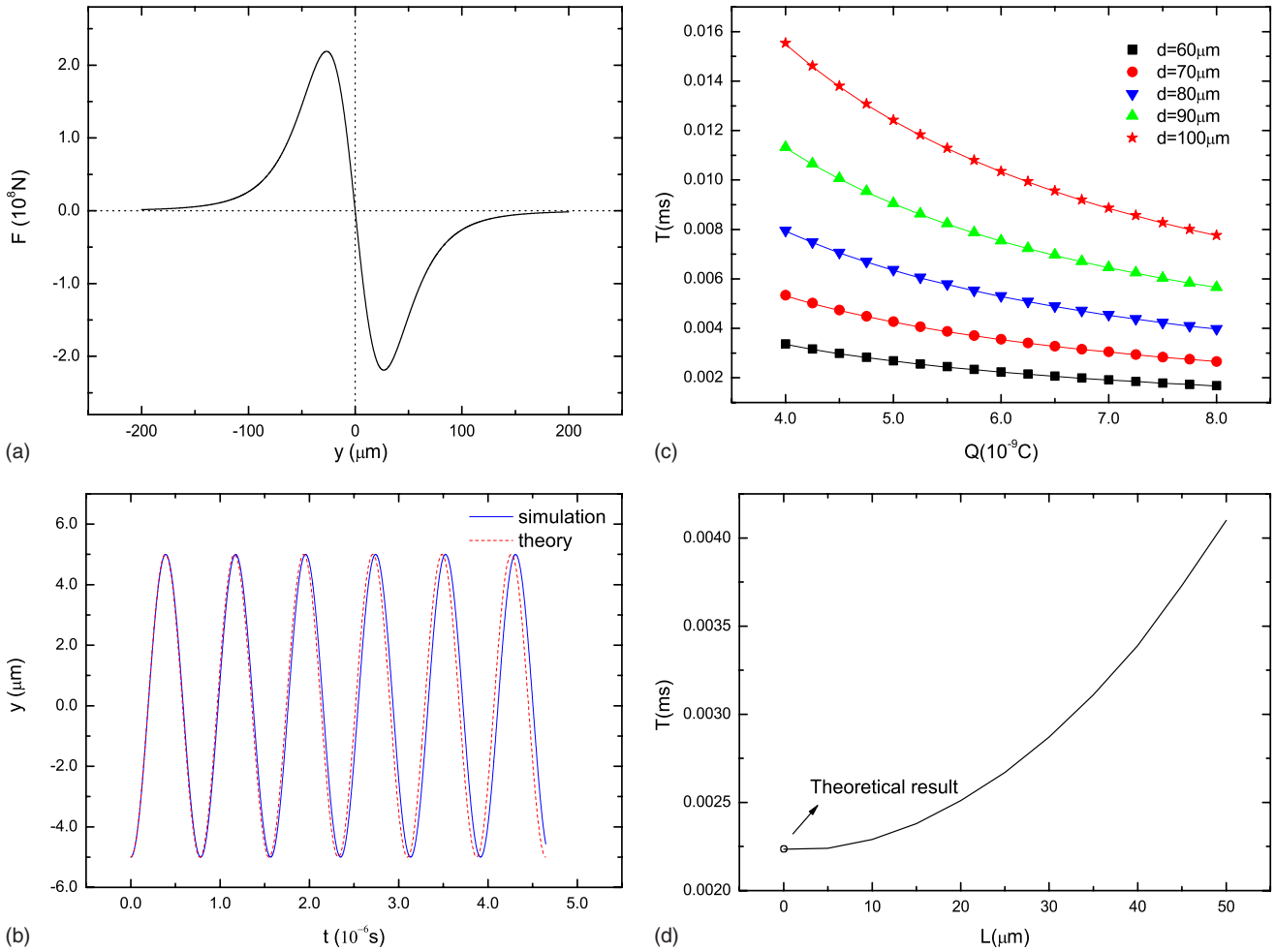

FIG. 2. (Color online) (a) The DEP force F along the microchannel acting on microparticle P as a function of its displacement y according to Eq. (2), in the presence of Q on microelectrode A only. Parameters: $\rho=3.75\times10^3$ kg/m^3, $a=1$ μm, $Q=0.8\times10^{-8}$ C, $d=60$ μm, $\varepsilon_2=9\varepsilon_0$, and $\varepsilon_1=\varepsilon_0$. (b) Oscillative behaviors of microparticle P for a small oscillation amplitude, obtained by using numerical and theoretical calculations, respectively. Parameters: $d=50$ μm, (for numerical approach) $L=5$ μm, other parameters are the same as in (a). (c) Period T of microparticle P oscillating in simply harmonic motions as a function of charge Q applied on A, for different separations d, calculated both numerically and theoretically. The symbols denote the results obtained by the numerical calculations, and the straight lines are the corresponding theoretical calculations. Perfect agreement between the numerical calculation and theory is clearly shown. Parameters: $L=5$ μm for the numerical calculations and other parameters are the same as those used in (a). (d) Period T vs oscillation amplitude L, obtained numerically. The marked point refers to the extreme, which is simply harmonic oscillation (at this point, theoretical and numerical results are exactly the same). Parameters: $Q=6\times10^{-9}$ C, $d=60$ μm, and other parameters are the same as those used in (a).

that simply harmonic oscillations come to appear only for small amplitudes.

With the analysis above, it is easy to understand that when we have Q on microelectrode A and with equal q on microelectrodes B and C, with the condition of $q \ll Q$, all properties remain the same as the situation with only Q. As a demonstration, we compare the force field between the two in Fig. 3, which shows little deviation. Therefore, the oscillation of the particle has the same qualitative behaviors as demonstrated before.

In the sense of a oscillation with a fixed period T described here, this system can be used to record time,[24] which can also be achieved when $q \ll Q$ for the three microelectrode system.

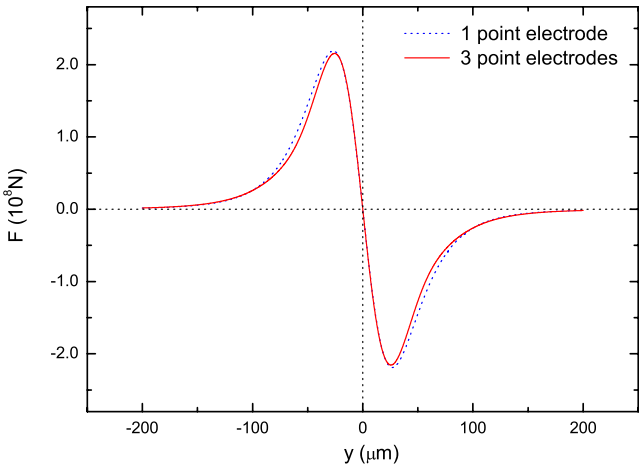

FIG. 3. (Color online) The DEP force F along the microchannel acting on microparticle P as a function of its displacement y in the presence of the three microelectrodes A, B, and C. The force obtained for the case with microelectrode A only is also plotted for comparison. Parameters: $Q=0.8\times10^{-8}$ C, $d=60$ μm, $q=2\times10^{-10}$ C, $r=50\sqrt{2}$ μm, and $\theta=45°$.

B. A random number generator

We now consider the case with q applied on both microelectrodes B and C, for which the system can have two stable points. To proof this, we get a force field according to this

two electrode configuration system (but for the complicated analytical result, we do not include it herein). The numerical solution of the force acting on microparticle P as a function of its position is shown in Fig. 4(a). Three zero-value points M, N, and O appear, among which M and N correspond to two stable equilibrium positions, while O serves as an unstable equilibrium position.

The distance h between the point M (or N) and the origin O depends on only the position of microelectrodes B and C [see Fig. 4(b)]. Here the distance h is displayed as a function of r for different angles θ, calculated numerically. And the slope h/r versus θ in view of the linear relation is shown in Fig. 4(c). The linear relation between h and r shows the scale-free property of this system. It can be seen that the proportion constant h/r is caused to monotonically increase as the angle θ increases, which converges to 1 as $\theta \rightarrow 90°$. The zero-value point (25.3, 0) shown in Fig. 4(c) represents the critical value of θ for a transition between a monostable system and a bistable one (which is 25.3°). That is, for cases with $\theta < 25.3°$, the corresponding force has only one zero-value point, indicating only one maximum of electric field along the y axis.

Then we move to look into the role microelectrode A plays in the system. In the situation of q always applied on, when microelectrode A is also on (with charge q and $q \ll Q$), the microparticle will be located at O. Then discharge of microelectrode A releases the microparticle from O, and thus enables a random displacement of P caused by Brownian motion. The displacement will be amplified even larger, and the microparticle will be eventually located at one of M and N (because of drag forces), with equal probability. We can define 0 and 1 of the location M and N, and thus the system can be utilized as a binary random number generator: Shift-off of microelectrode A produces a binary number 0 or 1, and shift-on of A resets the system.

To show the two processes, we take the viscosity $\eta = 8.0 \times 10^{-3}$ kg/(m s) and $\varepsilon_1 = 1.8 \times 10^{-11}$ F/m (namely, $2.03\varepsilon_0$). Then, we are allowed to obtain microparticle P's motion trajectory by solving its motion equation

$$m\frac{d^2y}{dt^2} = F - 6\pi a\eta\frac{dy}{dt}, \tag{6}$$

where F takes a form that can be obtained similarly with Eq. (3), but more complex due to two q's contributions. In this equation, we have used the Stokes formula to represent the expression for the drag force. Figure 5(a) shows the motions of P after microelectrode A is shifted off, given that its initial state is at rest in position O. Figure 5(b) shows the reverse action of microparticle P after the shift-on of A, with the initial state of P resting at one of the two points M or N. We can see that in both cases, for the small scale of the microparticle and a comparatively large viscosity chosen in the calculation (which refers to a very small Reynolds number meaning the viscous force typically overwhelms inertial forces[25]), microparticle P cannot move across the stable position, and its kinetic energy dropping to zero immediately when its driving force (the DEP force in this context) drops to zero. In the case of shift-off, microparticle P at O will move along either the $+y$- or $-y$-direction, determined by the effect of the Brownian motion. In other words, at a specific time, the stochastic force acting on microparticle P arising from the bombardment of liquid molecules is nonsymmetri-

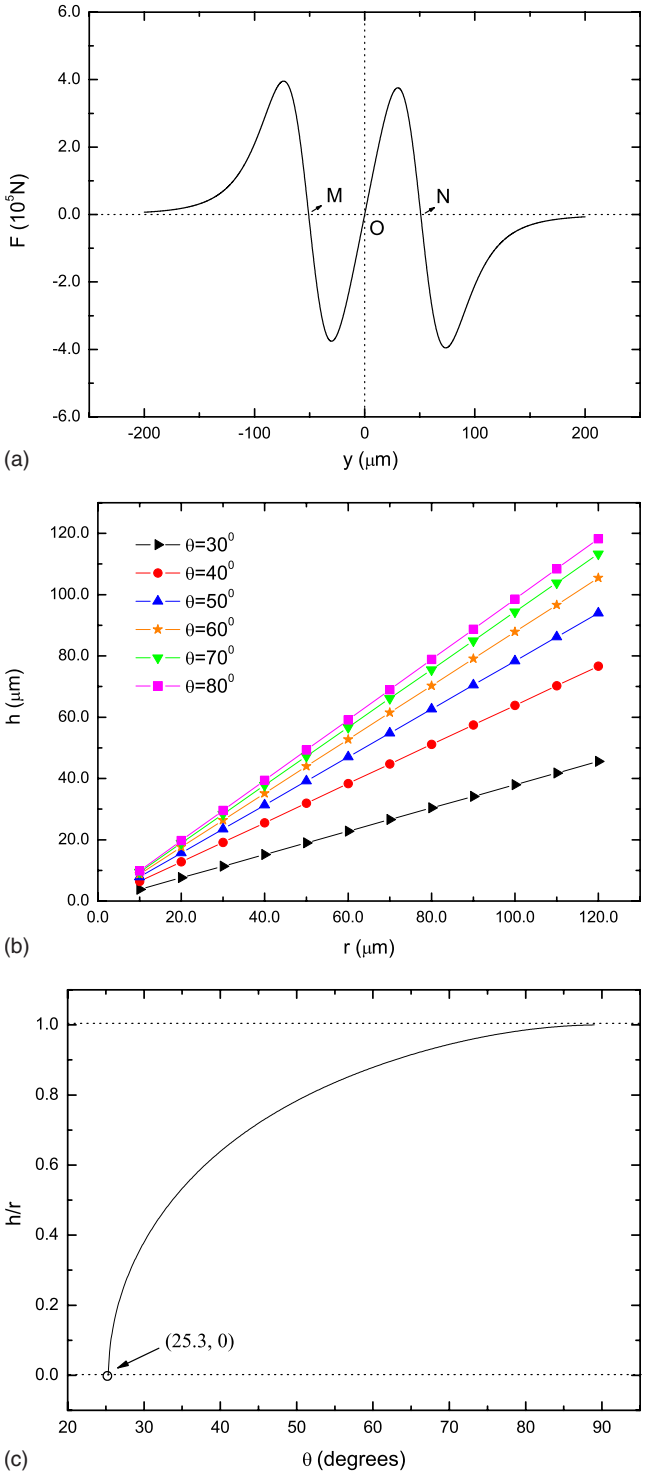

FIG. 4. (Color online) (a) The DEP force F along the microchannel acting on microparticle P as a function of its displacement y, in the presence of q on microelectrodes B and C only. Parameters: $q = 2 \times 10^{-10}$ C, $r = 50\sqrt{2}$ μm, $\theta = 45°$, and other parameters are the same as those used in Fig. 2(a). (b) The distance h between the center O of the microchannel and the stable position as a function of separation r for different angles θ. (c) The ratio of h/r as a function of angle θ. The point (25.3, 0) corresponds to the critical value $\theta = 25.3°$ above which a bistable system can be achieved. For plotting the two panels, except for $Q = 0$, no other parameters have been adopted. In other words, the two panels (c) and (d) are independent of the explicit values for q, ε_1, and ε_2.

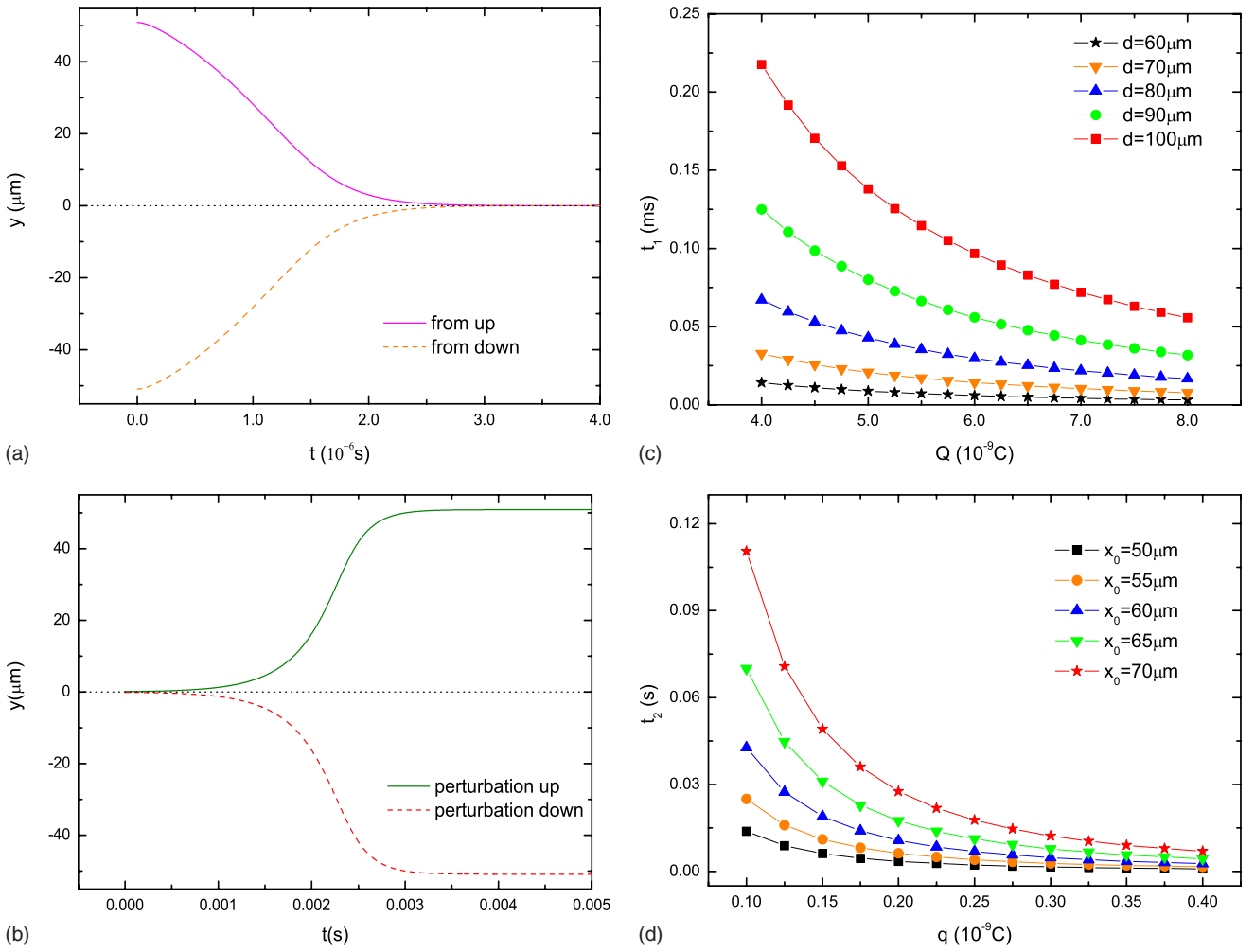

FIG. 5. (Color online) (a) The motion of microparticle P, triggered by an off-to-on shift of microelectrode A. (b) The motion of microparticle P, triggered by an on-to-off shift of microelectrode A. Parameters for (a) and (b): $\rho=3.75\times10^3$ kg/m^3, $a=1$ μm, $\eta=8.0\times10^{-3}$ kg/(m s), $\varepsilon_1=1.8\times10^{-11}$ F/m, $\varepsilon_2=9\varepsilon_0$, $Q=0.8\times10^{-8}$ C, $d=60$ μm, $q=2\times10^{-10}$ C, $r=50\sqrt{2}$ μm, and $\theta=45°$. (c) Typical time t_1 vs Q for different distances d. (d) Typical time t_2 vs q for various separations r (which here is equivalently represented by x_0 in Fig. 1) at $\theta=45°$. For (c) and (d) parameters are the same as those used in (a).

cal, which can cause the microparticle in the microchannel to move along either the $+y$- or $-y$-direction.

Two response times t_1 and t_2 are the key parameters for the random number generator, referring to the time of generating a random number and that of resetting the system, respectively. We plot t_1 versus Q for different distances d [see Fig. 5(c)] and t_2 versus q for various distances r (which here is equivalently represented by x_0 in Fig. 1) [see Fig. 5(b)]. In calculating t_2, we set the initial displacement caused by the Brownian force to be 0.1 μm. For both cases, t_1 and t_2 decrease monotonically with respect to an increase in applied charges (Q or q) and/or a decrease in separations (d or r). It can be easily understood that when the viscosity η increases, the dissipating speed of microparticle P's kinetic energy is caused to increase naturally and the t_1 and t_2 should increase accordingly. Such figures are not shown herein.

C. A flip-flop

With the two bistable points produced by microelectrodes B and C with charge q, a flip-flop device can also be proposed. Here, an instant shift-on of microelectrode A can toggle the microparticle from one side to the other. We denote the acting time of the toggling signal to be t_{tog}. If the time t_{tog} is appropriately adjusted, microparticle P will be toggled to the other side.

To show the range of valid toggling time, we plot Fig. 6 as explanations. First, P's motion due to a permanent off-on shift is plotted for comparison [see Fig. 6(a)]. Apparently, when A is charged with Q at $t=0$, microparticle P is immediately induced a driving force toward the origin. P will not rest at origin O before several times of damped vibrations. We observe twice of its oscillations in Fig. 6(a). In principle, for each oscillation, there is a time span in which the shift-off of microelectrode A can toggle the microparticle P to the other side successfully. That means, at the time when Q is released, the microparticle has been toggled to be in a proper position with a proper momentum that can further drive the microparticle toward the other side. However, for obviousness and simplicity, we only take into account for the time span within the first damped oscillation. The time range [0.39,0.68] μs, marked in Fig. 6(a) just corresponds to the range of valid toggling times t_{tog} that allow one to successfully toggle microparticle P from 0 to 1 states. Figures 6(b) and 6(c) display the two extreme cases for $t_{tog}=0.39$ μs and

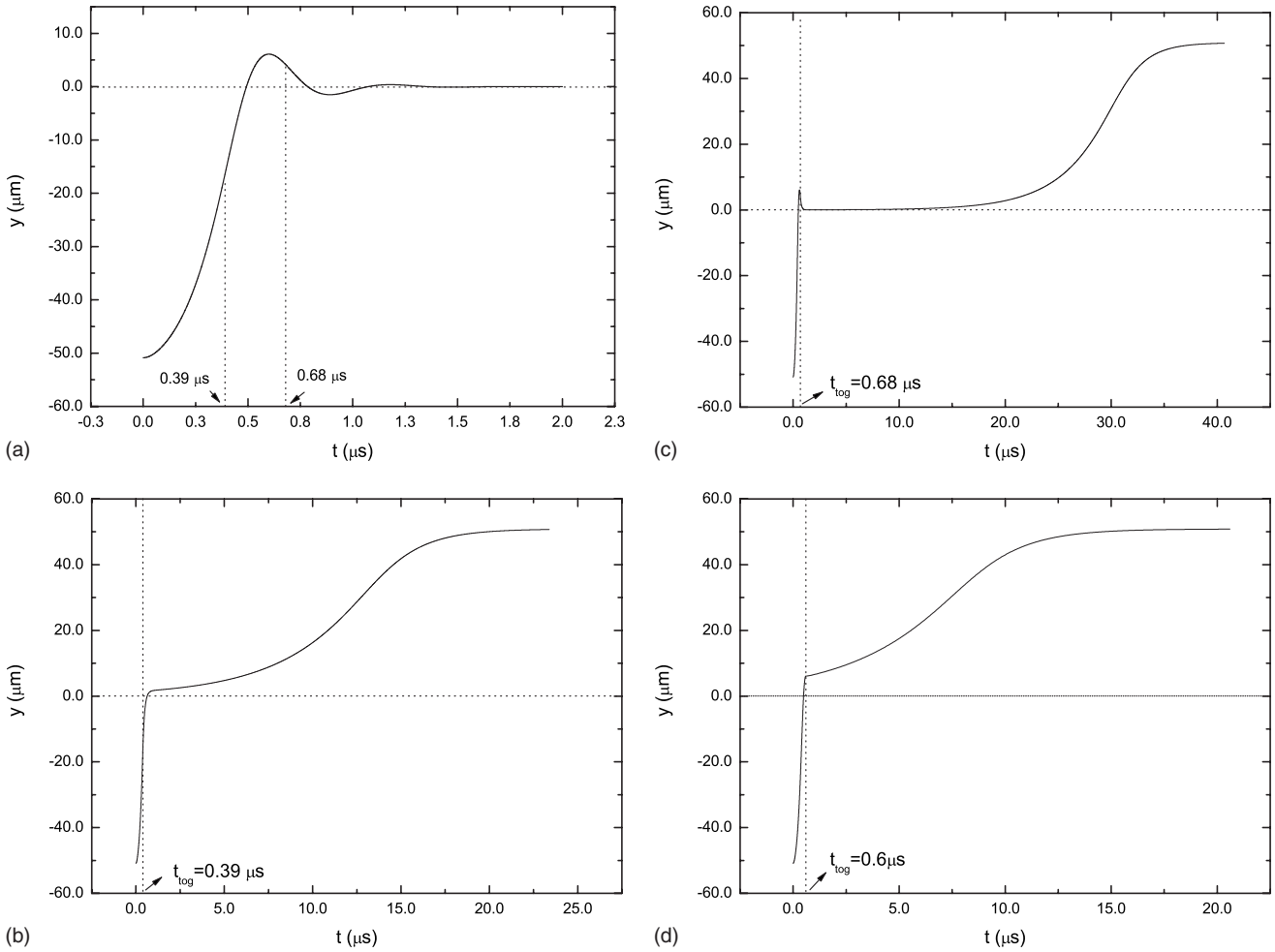

FIG. 6. (a) The motion of microparticle P in the presence of microelectrode A with charge Q acting for $t \geq 0$. The time range $[0.39\ \mu s, 0.68\ \mu s]$ is indicated, and the flip-flop function holds only for $t_{tog} \in [0.39\ \mu s, 0.68\ \mu s]$. (b) The flip-flop process with the minimum toggling time $t_{tog}=0.39\ \mu s$. (c) The flip-flop process with the maximum toggling time $t_{tog}=0.68\ \mu s$. (d) The flip-flop process with $t_{tog}=0.6\ \mu s$ (which is the acting time of the toggling signal). Parameters: $Q=2\times10^{-8}$ C and $q=2\times10^{-9}$ C. Other parameters are the same as those used in Fig. 5.

$t_{tog}=0.68\ \mu s$, respectively, while Fig. 6(d) shows the case falling between them. The reverse motion from 1 to 0 states is similar and thus is not detailed herein.

Also, we list here several other potential applications on this system. First, on and off states can be defined to control reactions. Also more than one microparticle (or even more than one kind of microparticles) can be considered into the system, and a shift-on of microelectrode A forces all the microparticles together, possibly causing a reaction. And it is even more interesting when the microparticle P is replaced with a droplet. However, as for the length of this manuscript, we will not include these considerations here.

IV. CONCLUSION AND DISCUSSIONS

To sum up, we have investigated a DEP-based microchannel system, and proposed in detail three possible applications on it. Analyses on both theoretical and numerical sides are both conducted, which yields proposals on potential applications of a microparticulate clock, a random number generator, a flip-flop device, and other possibilities.

It should be remarked that though this microchannel system introduces a concept of computation and multifunction by implementing a microparticle into LOC systems, it is by no means a completed design for an instant practical use. Questions remain on the side of engineering. First, the export of information for practical LOC use based on this microchannel system remains as an open question. That is, for a practical clock, the information of timing should be exported. Also, information of 0 and 1 should also be exported for a next unit of calculation for the random number generator and the flip-flop. Second, to achieve a fast response time, in our calculations, the magnitude of the DEP force exerted on the microparticle is up to the scale of 10^8 N, which is a quite large value compared with usual forces existing in most microfluidic experiments. Nevertheless, such a value can indeed be achieved as long as the corresponding charge application can be realized experimentally. In addition, for the convenience of experimental realization, the three point microelectrodes can be replaced with three line microelectrodes. Functions and qualitative results will remain unchanged due to the symmetry of the system.

ACKNOWLEDGMENTS

We thank Dr. C. F. Chou and Dr. M. Karttunen for fruitful discussions. We acknowledge the financial support by the National Natural Science Foundation of China under Grant

Nos. 10604014 and 10874025, the Shanghai Education Committee, the Shanghai Education Development Foundation ("Shu Guang" project under Grant No. 05SG01), the Scientific Research Foundation for the Returned Overseas Chinese Scholars, State Education Ministry, China, Chinese National Key Basic Research Special Fund under Grant No. 2006CB921706, and National Fund for Talent Training in Basic Science (Grant No. J0730310).

[1]H. Craighead, Nature (London) **442**, 387 (2006).
[2]J. Borowsky and G. E. Collins, Analyst (Cambridge, U.K.) **132**, 958 (2007).
[3]J. Do and C. H. Ahn, Lab Chip **8**, 542 (2008).
[4]T. Thorsen, S. J. Maerkl, and S. R. Quake, Science **298**, 580 (2002).
[5]J. M. Ramsey, J. P. Alarie, S. C. Jacobson, and N. J. Peterson, *Micro Total Analysis Systems* 2002, edited by Y. Baba, S. Shoji, and A. J. van den Berg, (Kluwer Academic Publishers, Dordrecht, 2002), Vol. 1, p. 314.
[6]M. Prakash and N. Gershenfeld, Science **315**, 832 (2007).
[7]M. W. Toepke, V. V. Abhyankar, and D. J. Beebe, Lab Chip **7**, 1449 (2007).
[8]H. A. Pohl, *Dielectrophoresis* (Cambridge University Press, New York, 1978).
[9]M. P. Hughes, Electrophoresis **23**, 2569 (2002).
[10]N. Markarian, M. Yeksel, B. Khusid, K. Farmer, and A. Acrivos, Appl. Phys. Lett. **82**, 4839 (2003).
[11]T. P. Hunt, H. Lee, and R. M. Westervelt, Appl. Phys. Lett. **85**, 6421 (2004).
[12]C. Z. Fan, J. P. Huang, and K. W. Yu, J. Phys. Chem. B **110**, 25665 (2006).
[13]I. Barbulovic-Nad, X. Xuan, J. S. H. Lee, and D. Li, Lab Chip **6**, 274 (2006).
[14]T. Sun, H. Morgan, and N. G. Green, Phys. Rev. E **76**, 046610 (2007).
[15]B. H. Lapizco-Encinas and M. Rito-Palomares, Electrophoresis **28**, 4521 (2007).
[16]Y. Kang, D. Li, S. A. Kalams, and J. E. Eid, Biomed. Microdevices **10**, 243 (2008).
[17]R. Hölzel, N. Calander, Z. Chiragwandi, M. Willander, and F. F. Bier, Phys. Rev. Lett. **95**, 128102 (2005).
[18]L. Zheng, S. Li, J. P. Brody, and P. J. Burke, Langmuir **20**, 8612 (2004).
[19]T. B. Jones, K. L. Wang, and D. J. Yao, Langmuir **20**, 2813 (2004).
[20]L. Dong, J. P. Huang, and K. W. Yu, J. Appl. Phys. **95**, 8321 (2004).
[21]T. B. Jones and G. W. Bliss, J. Appl. Phys. **48**, 1412 (1977).
[22]Z. Qiu, N. Markarian, B. Khusid, and A. Acrivos, J. Appl. Phys. **92**, 2829 (2002).
[23]T. B. Jones, *Electromechanics of Particles* (Cambridge University Press, New York, 1995).
[24]Y. Gao, W. J. Tian, W. Wang, and J. P. Huang, Appl. Phys. Lett. **92**, 122902 (2008).
[25]T. M. Squires and S. R. Quake, Rev. Mod. Phys. **77**, 977 (2005).